Performance analysis of IR-UWB in multi-user environment

Fatma Kharrat-Kammoun*, Christophe J. Le Martret†, and Philippe Ciblat*
*Institut TELECOM, TELECOM ParisTech, Paris, France
Email: fkharrat@enst.fr, philippe.ciblat@enst.fr
†Thales Communications, Colombes, France
Email: christophe.le_martret@fr.thalesgroup.com

***Abstract*— In Impulse Radio Ultra Wide Band (IR-UWB) based systems, we show that the Multi-User Interference (MUI) assuming fixed spreading codes can be well approximated by a Generalized-Gaussian Distribution (GGD). Then, we derive an accurate closed-form expression of the approximation for the Average Error Probability (AEP) in both Direct-Sequence (DS) and Time-Hopping (TH) multiple access context. From this approximation, we are able to characterize and to select the set of codes minimizing the AEP for both multiple access techniques. The merit of each multiple access technique is then analyzed: we especially prove that the probability to find an optimal pair of codes goes to one when increasing the number of chips per symbol with TH technique whereas this probability goes to zero with DS technique. Numerical illustrations confirm our claims.**

I. Introduction

UWB technology is a viable solution for short range and indoor wireless applications. Its low power consumption allows to reduce the interference between UWB and other wireless systems and its high data rates enables UWB to support multiple users within the same radio channel. TH and DS are the two popular multiple access techniques that are proposed for UWB systems combined with different modulation schemes, such as Pulse Position Modulation (PPM), Pulse Amplitude Modulation (PAM) and On-Off Keying (OOK) [1]. Performance analysis of multi-user UWB systems with different multiple access and modulation schemes has been already conducted in the literature in the following way. The first studies assumed a Gaussian approximation for the MUI and then the derivation of the error probability needs simply the determination of the MUI variance [2], [3]. Nevertheless, it was shown later in [4] that the Gaussian approximation overestimates the performance of a standard Rake receiver and therefore it is inaccurate to model the MUI. The Gaussian approximation inaccuracy is also exhibited by simulations in [5]. Recently, an exact AEP has been provided in [6] for both TH and DS UWB systems. Their derivations are based on the study of the characteristic function of the MUI. The obtained AEP is accurate but its expression is still complex and does not provide insight about the influence of design parameters (such as the multi-user codes). Actually if we would like to obtain a simple approximated AEP closed-form expression, we need to carefully approximate the MUI distribution. In [7], [8], [9], [10], [11], [12], it was shown that either the GGD or the Gaussian mixture or α-stable distributions are relevant choices to describe the MUI distribution. In [7], the AEP expression based on GGD approximation (for TH technique and PAM modulation) is provided and involves the second and fourth order moments of the MUI. Moreover their expression does not explicitly depend on the multiple access codes since the authors averaged the MUI moments with respect to the multiple codes. Notice that, in the context of either GGD or Gaussian mixtures or α-stables distribution, new powerful receivers can be carried out by using a soft limiter device [8], [9], [14]. These new receivers will not be considered in this paper which focuses on the performance of the standard Rake receiver. Concerning the choice of the multiple access codes, one can mention the work of [15] which proposed to minimize the second order moment of the MUI, in fact the variance, with respect to the multiple access codes in order to optimize the performance for TH and DS UWB systems. Intuitively, minimizing the MUI variance is necessary but not sufficient since the AEP depends on the high order statistics. Besides, in this paper, we will prove that a second criterion related to the fourth order moment has to be considered in order to really minimize the impact of the multiple access on the system performance. The first criterion is the MUI variance described in [15].

The contribution of the paper are threefold:

- Assuming that the MUI is generalized-Gaussian distributed, *we derive an accurate closed form expression for the AEP in function of the multiple access codes for both TH and DS multiple access techniques*.
- From the obtained AEP approximation, we are able to exhibit criteria that the multiple access codes have to minimize in order to optimize the AEP for both access techniques. Minimizing such criteria leads the *optimal multiple access to satisfy some constraints that are characterized in this paper*. The comparison of the obtained code constraints to those illustrated in [15] shows that the variance minimization is insufficient to optimize the performance for PAM TH UWB systems; whereas it achieves the best one with PPM TH and PAM DS UWB systems.
- In [6], the authors use their AEP closed-form expression to compare both TH and DS access techniques

This work was supported by ANR grant for project called RISC. This material has been partially presented at PIMRC'2008.

assuming random codes and same data rate for both systems while the captured energy with DS is higher than that with TH technique. Based on their numerical results, they shown that PAM DS outperforms PAM TH UWB systems and that PPM TH UWB systems achieve the worst performance. In this paper, we compare both access techniques combined to a PAM modulation while keeping fixed and judiciously choosing the access codes. These codes, called optimal codes, are selected in such a way to minimize the contribution of the multiple access impairments. However, *a theoretical study of the optimal codes distribution shows that the probability that a pair of codes be optimal goes to 0 when increasing the number of chips per symbol with DS technique. Fortunately, this probability goes to 1 when employing TH technique*. So, finding a pair of optimal codes is not guaranteed for DS UWB whereas it is for TH UWB systems. Based on simulation results, we show that TH scheme (using well-chosen codes, thus optimal pair of codes) outperforms DS one (using well-chosen codes but not necessary optimal pair of codes) while assuming same data rate and same captured energy.

This paper is organized as follows. In Section II, we introduce the transmitted signal model for PAM TH, PPM TH and PAM DS IR-UWB systems. The considered channel model and the rake receiver structure are described as well. In Section III, assuming the codes to be fixed, we derive the AEP in closed-form for the three analyzed systems using the generalized Gaussian approximation whose parameters are evaluated in terms of the multiple access codes. In Section IV, we present criteria that the codes have to satisfy in order to improve the performance. The study of the optimal codes distribution is done in Section V for both DS and TH techniques. Section VI is devoted to numerical illustrations: we validate our GGD based approximation and we also inspect the impact of the codes choice on the performance; we show that the AEP significantly decreases when codes are selected as suggested in Section IV; a comparison of PAM TH and DS UWB systems is carried out. Conclusions are given in Section VII.

II. Signal model

We consider an IR-UWB system with either TH or DS as a code division multiple access technique. Both PAM and PPM modulations can be used for TH technique; whereas PAM modulation is only considered for DS technique. Let N_u be the number of active users in the network. Each user transmits information asynchronously through a multipath channel. Using the Developed Time Hopping (DTH) code for TH technique [15], the transmitted signal depends only on the applied modulation as follows.

For **PAM** modulation, the transmit signal from user n is expressed similarly for DS and TH techniques:

$$s_n(t) = \sum_{i=-\infty}^{\infty} d_n(i) \sum_{j=0}^{N_c-1} c_n(j) w(t - iT_s - jT_c - \theta_n), \quad (1)$$

where

- T_s is the symbol time where each symbol consists of N_c chips of duration T_c each one,
- $w(t)$ is the normalized impulse of duration $T_w \ll T_c$,
- $d_n(i)$ are the information symbols of user n, assumed to be independent and identically distributed. The symbols $d_n(i)$ belong to the set $\{-1, 1\}$,
- $\{c_n(j)\}_{j=0}^{N_c-1}$ is the multiple access code associated with user n, with either $c_n(j) \in \{-1, 1\}$ for DS code in DS scheme or $c_n(j) \in \{0, 1\}$ for the DTH code in TH scheme,
- θ_n is the time asynchronism that is assumed to be a uniformly distributed within $[0, T_s]$.

Notice that $N_c = N_s N_h$ where N_s is the number of frames and N_h is the number of chips per frame in TH scheme. In DS scheme, the number N_h is equal to 1.

For **PPM** modulation, the expression of the TH transmit signal, using DTH code, is:

$$s_n(t) = \sum_{i=-\infty}^{\infty} \sum_{j=0}^{N_c-1} c_n(j) w(t - iT_s - jT_c - \delta d_n(i) - \theta_n), \quad (2)$$

where $\delta \ll T_c$ is the PPM shift and the symbols $d_n(i)$ belong to $\{0, 1\}$.

The receiver input signal is the sum of the attenuated and delayed transmit signals from the different users. Its expression is given by

$$y(t) = \sum_{n=1}^{N_u} \sqrt{P_n} \left(\sum_{k=1}^{N_p} A_n^k s_n(t - \tau_n^k) \right) + n(t), \quad (3)$$

where A_n^k and τ_n^k are the amplitude and the delay of the k^{th} path between the user n and the receiver, N_p is the number of paths assumed to be the same for all the users, P_n is the captured power, and $n(t)$ is an additive zero-mean white Gaussian noise.

The multipath channel model we employ is that proposed generally for UWB systems. The amplitude A_n^k is usually assumed to be dependent on the delay τ_n^k as $A_n^k = a_n^k f(\tau_n^k)$, where a_n^k are independent zero-mean random variables (rv) and $f(\cdot)$ is a function which indicates the variation of the amplitude according to the delay. The information about random captured powers is provided by the set $\{P_n\}_{n=1,\cdots,N_u}$. The rv τ_n^k are assumed to be independent between users but are usually correlated for a given user. The distribution of the variables τ_n^k and a_n^k are provided in the IEEE 802.15.3a standard [16]. When only one cluster is considered (which is not restrictive as mentioned in [17]), the delay τ_n^k follows a Poisson distribution. The attenuation $a_n^k = p_n^k \cdot \beta_n^k$, where $p_n^k \in \{\pm 1\}$ are equiprobable and β_n^k are log-normal rv. The function $f(\cdot)$ is defined by $f(\tau_n^k) = e^{-\tau_n^k/2\gamma}$, where γ is the path power-decay time.

Without loss of generality, the user of interest is assumed to be the user 1. We consider the rake receiver of user 1, commonly used for multipath channel systems, with $L_r \leq N_p$ fingers. We also assume that the receiver is synchronized (i.e., $\theta_1 = 0$) and has the perfect knowledge of the channel multipaths. Thus, the rake receiver output for the first symbol

is

$$z = \sum_{\ell \in \mathcal{L}} A_1^\ell \int_0^{T_s} y(t + \tau_1^\ell) \cdot v_1(t) \mathrm{d}t, \quad (4)$$

where $v_1(t) = \sum_{j=0}^{N_c-1} c_1(j) v(t - jT_c)$ is the template signal associated with user 1. Notice that $v(t) = w(t)$ for PAM modulation and $v(t) = w(t) - w(t-\delta)$ for PPM modulation, and $\mathcal{L}$ is the selected subset paths with Card($\mathcal{L}$)=L_r. Using Eqs. (3)-(4), the rake receiver output ([15]) is

$$z = \sum_{\ell \in \mathcal{L}} A_1^\ell \sum_{n=1}^{N_u} \sqrt{P_n} \sum_{k=1}^{N_p} A_n^k y_{k,\ell,n}(\theta_n) + \eta, \quad (5)$$

where $\eta = \sum_{\ell \in \mathcal{L}} A_1^\ell \int_0^{T_s} n(t + \tau_1^\ell) v_1(t) \mathrm{d}t$ is the filtered Gaussian noise. The expression of the term $y_{k,\ell,n}(\theta_n)$ depends on the modulation format ([15]) as follows:

$$\begin{aligned} y_{k,\ell,n}(\theta_n) &= \tilde{r}(\epsilon_n^{k,\ell}, q_n^{k,\ell}, Q_n^{k,\ell}) \\ &+ \tilde{r}(\epsilon_n^{k,\ell} - T_c, q_n^{k,\ell} + 1, Q_n^{k,\ell}), \ (\textbf{PAM}) \quad (6) \\ y_{k,\ell,n}(\theta_n) &= \tilde{r}_1(\epsilon_n^{k,\ell}, q_n^{k,\ell}, Q_n^{k,\ell}) \\ &+ \tilde{r}_1(\epsilon_n^{k,\ell} - T_c, q_n^{k,\ell} + 1, Q_n^{k,\ell}), (\textbf{PPM}) \quad (7) \end{aligned}$$

where $Q_n^{k,\ell} = \lfloor \Delta_n^{k,\ell}/T_s \rfloor$, $q_n^{k,\ell} = \lfloor (\Delta_n^{k,\ell} - Q_n^{k,\ell} T_s)/T_c \rfloor$ and $\epsilon_n^{k,\ell} = \Delta_n^{k,\ell} - Q_n^{k,\ell} T_s - q_n^{k,\ell}$ with $\Delta_n^{k,\ell} = \theta_n + \tau_n^k - \tau_1^\ell$. We also put

$$\begin{aligned} \mathcal{C}_{m,n}^-(q) &= \sum_{k=0}^{q-1} c_m(k) c_n(k-q), \\ \mathcal{C}_{m,n}^+(q) &= \sum_{k=q}^{N_c-1} c_m(k) c_n(k-q), \quad (8) \end{aligned}$$

$r(s) \rightleftharpoons \int_{-\infty}^{+\infty} w(t) w(t-s) \mathrm{d}t$, $r_1(s) \rightleftharpoons \int_{-\infty}^{+\infty} (w(t) - w(t-\delta)) w(t-s) \mathrm{d}t$, $\tilde{r}(\epsilon, q, Q) \rightleftharpoons r(\epsilon) \left[d_n(-Q) \mathcal{C}_{1,n}^+(q) + d_n(-Q-1) \mathcal{C}_{1,n}^-(q) \right]$ and $\tilde{r}_1(\epsilon, q, Q) = \mathcal{C}_{1,n}^+(q) r_1(\epsilon + \delta d_n(-Q)) + \mathcal{C}_{1,n}^-(q) r_1(\epsilon + \delta d_n(-Q-1))$.

Notice that the rake receiver output given by Eq. (5) can be decomposed as [15]:

$$z = z_U + z_I + z_M + \eta, \quad (9)$$

where

- z_U is the Useful part of user 1 signal, $z_U = \sqrt{P_1} \sum_{\ell \in \mathcal{L}} (A_1^\ell)^2 y_{\ell,\ell,1}(0)$,
- z_I is the Inter-symbol interference from user 1, $z_I = \sqrt{P_1} \sum_{\ell \in \mathcal{L}} A_1^\ell \sum_{k \neq \ell = 1}^{N_p} A_1^k y_{k,\ell,1}(0)$,
- z_M is the Multi-user interference, $z_M = \sum_{\ell \in \mathcal{L}} A_1^\ell \sum_{n=2}^{N_u} \sqrt{P_n} \sum_{k=1}^{N_p} A_n^k y_{k,\ell,n}(\theta_n)$.

Unlike z_I and z_M, the useful part z_U and the noise η do not depend on the multiple access codes. If the number of users is large enough, it has been remarked that the term z_I can be neglected compared to the term z_M [2], [13]. In the sequel, for the sake of simplicity, on the one hand, we assume that $z_I = 0$ and the selected paths are normalized, i.e. $\sum_{\ell \in \mathcal{L}} (A_n^\ell)^2 = 1 \ \forall n$, and on the other hand, we consider the set of captured powers fixed, i.e., the obtained closed-form expression will depend on the realization of $\{P_n\}_{n=1,\cdots,N_u}$.

III. AEP approximation based on Generalized Gaussian distribution

The first works dealing with the performance of UWB systems assumed that the MUI was a Gaussian distributed random variable [2], [3]. Thus, the evaluation of the error probability requires simply the computation of the variance of the rv $z_M + \eta$. Unfortunately, in [4], [5], [18], [19], the authors criticize the validity of the Gaussian approximation to model the MUI for UWB systems. Later, in [20], the authors studied the MUI Gaussianity condition for TH access technique where the number of users N_u and the number of chips $N_c = N_s N_h$ grow toward the infinity at the same rate, *i.e.*, N_u/N_c goes toward a positive constant. Thanks to the central limit theorem, they have proven that the Gaussian approximation is valid if and only if the ratio N_s/N_h converges toward a positive constant.

Recently, it has been proposed to use the GGD to describe the MUI distribution in TH IR-UWB system [7] in AWGN context. We remind that the GGD writes as follows [22]:

$$p(x) = \frac{\sqrt{\Gamma_c(3/\alpha)}}{2\sigma \sqrt{\Gamma_c(1/\alpha)} \Gamma_c(1 + 1/\alpha)} e^{-\left| \frac{\sqrt{\Gamma_c(3/\alpha)}}{\sigma \sqrt{\Gamma_c(1/\alpha)}} x \right|^\alpha}, \quad (10)$$

where σ^2 is the variance, $\alpha > 0$ is the so-called shape parameter, and $\Gamma_c(.)$ is the (complete) Gamma function. Remark that when $\alpha = 2$, $p(x)$ corresponds to a Gaussian distribution. To ensure that the GGD remains accurate to model the MUI when DS technique is employed and when multipath channel (described in Section II) is assumed, we compare the empirical MUI distribution to that described by Eq. (10) where α and σ^2 are obtained empirically. In Figs. 1 and 2, we illustrate the MUI distribution for a PAM DS UWB system in AWGN context and for a PAM TH UWB system assuming a multipath channel and 32 active users respectively.

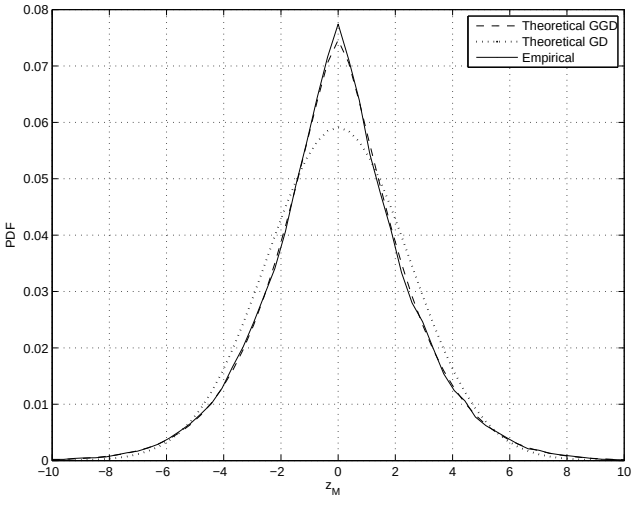

Fig. 1. Comparison of the empirical MUI PDF to those based on the GGD and the Gaussian distribution (GD) for PAM DS-UWB system in AWGN channel with $N_c = 5$, $T_c = 3$ ns and $N_u = 32$.

The implemented multipath channel is based on CM2 model which is described in [16]. In such a case, the PRake (Partial Rake) is employed where the receiver uses the first L_r paths

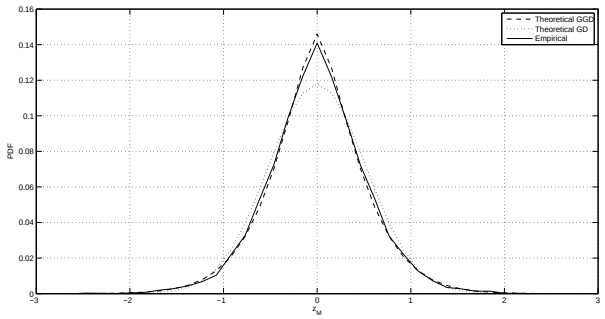

Fig. 2. Comparison of the empirical MUI PDF to those based on the GGD and the Gaussian distribution (GD) for PAM TH-UWB system in multipath channel with $N_c = 32$, $N_s = 2$, $T_c = 5$ ns, $N_u = 32$, $L_r = 3$ and $N_p = 20$.

among the all N_p received paths. The number of fingers and the paths are fixed to $L_r = 3$ and $N_p = 20$ respectively. Also, we plot in both figures the GGD and the Gaussian Distribution (GD). For both cases, it is clear that the MUI is well modeled by a GGD. However, a significant gap is noticed while comparing the empirical MUI distribution to that based on the standard Gaussian approximation. In the sequel, given the set of captured powers, we derive the AEP when the MUI is assumed to be GG distributed.

A. AEP approximation based on GGD

First of all, notice that the useful signal z_U in Eq. (9) depends on the modulation format. It is equal to $z_U = d_1(0)\sqrt{P_1}N_s$ for PAM modulation and $z_U = \sqrt{P_1}N_s\left(1 - r(\delta)\right)\left(1 - 2d_1(0)\right)$ for PPM modulation, where N_s is the repetition factor. Then, since the GGD is symmetric and both PAM and PPM modulations are equilikely, the AEP is given by:

$$\overline{P}_e = \mathrm{Prob}(\nu > \sqrt{P_1}N_s\xi) = \int_{\sqrt{P_1}N_s\xi}^{+\infty} p_\nu(x)dx, \qquad (11)$$

where $\xi = 1$ and $\xi = 1 - r(\delta)$ for PAM and PPM modulation respectively. We denote by $\nu = z_M + \eta$ the term disturbing the decision. Let $p_\nu(x)$ be its distribution.

As z_M is assumed to be GG distributed and as η is Gaussian distributed, i.e., GG distributed, we know that ν is also well approximated by a GGD. Indeed, in [21], one has been mentioned that the sum of two GG distributed variables can be approximated by a GG distributed variable as well. Consequently, the distribution of ν is described by Eq. (10) whose the shape parameter and variance are α and σ^2 respectively. Note that the expressions of α and σ^2 in terms of multiple access codes will be calculated in Section III-B. By replacing $p_\nu(x)$ in Eq. (11) with its expression in Eq. (10) and by doing tedious but straightforward algebraic manipulations (especially one change of variable $u = x^\alpha$), we get

$$\overline{P}_e = \frac{1}{2\alpha\Gamma_c(1+1/\alpha)}\Gamma_i\left[\frac{1}{\alpha}, \left(\frac{N_s\sqrt{P_1}\xi\sqrt{\Gamma_c(3/\alpha)}}{\sigma\sqrt{\Gamma_c(1/\alpha)}}\right)^\alpha\right] \qquad (12)$$

where $\Gamma_i[.,.]$ is the so-called incomplete Gamma function defined by $\Gamma_i[a,x] = \int_x^{+\infty} t^{a-1}\exp(-t)\mathrm{d}t$.

B. GGD parameters vs the multiple access codes

In the sequel, we denote by σ_M^2 and α_M the variance and the shape parameter of signal z_M respectively. Terms σ_η^2 and $\alpha_\eta = 2$ stand for the variance and the shape parameter of noise η respectively. Let us now focus on the derivation of σ^2 and α. As z_M and η are zero mean, so

$$\sigma^2 = \sigma_M^2 + \sigma_\eta^2. \qquad (13)$$

As mentioned [7], the shape parameter α of a GGD rv ν is related to the fourth and second order moment as follows

$$\alpha = F^{(-1)}\left(\frac{D^4}{\sigma^4}\right), \qquad (14)$$

where $D^4 = \mathbb{E}[\nu^4]$ and $F^{(-1)}(.)$ is the reciprocal function of $x \mapsto F(x) = \Gamma_c(5/x)\Gamma_c(1/x)/\Gamma_c^2(3/x)$. Let $D_M^4 = \mathbb{E}[z_M^4]$ and notice that $\mathbb{E}[\eta^4] = 3\sigma_\eta^4$. Like the second order moment, the fourth order moment of ν can be expressed in function of those of z_M and η as

$$D^4 = D_M^4 + 3\sigma_\eta^4 + 6\sigma_M^2\sigma_\eta^2. \qquad (15)$$

In order to determine perfectly the statistics of ν in terms of the multiple access codes, we only need to derive σ_M^2 and D_M^4 in terms of the multiple access codes. In [7], the average of σ_M^2 and D_M^4 over all the TH multiple access codes were evaluated. In our work, we remind that the multiple access codes are fixed since we would to select them according to the minimization of the obtained AEP approximation. Notice that the expectation for deriving the second and fourth order moments is achieved over the channel amplitude a_n^k, the symbol d_n, the asynchronism θ_n and the delay τ_n according to this order. Since the MUI depends on the modulation format and not directly on the access technique as shown in Eq. (9), we express σ_M^2 and D_M^4 only with respect to the applied modulation.

1) Closed-form expression of $\sigma_M^2 := \mathbb{E}_{a,d,\theta,\tau}[z_M^2]$: in [15] dedicated to TH technique, we have

$$\textbf{PAM:}\sigma_M^2 = \frac{\gamma_1}{T_s}\sum_{n=2}^{N_u} P_n\psi_n\sum_{q=0}^{N_c-1}\left[\mathcal{C}_{1,n}^{-2}(q) + \mathcal{C}_{1,n}^{+2}(q)\right], \qquad (16)$$

$$\begin{aligned}\textbf{PPM:}\sigma_M^2 &= \frac{1}{T_s}\sum_{n=2}^{N_u} P_n\psi_n\sum_{q=0}^{N_c-1} 2\left[\mathcal{C}_{1,n}^{-2}(q) + \mathcal{C}_{1,n}^{+2}(q)\right] \\ &\times \left(\gamma_1(0) - \gamma_1(\delta)\right) + \mathcal{C}_{1,n}^{+}(q)\mathcal{C}_{1,n}^{-}(q) \\ &\times \left[\gamma_1(0) - \gamma_1(2\delta)\right] \qquad (17)\end{aligned}$$

where $\gamma_1(s) = \int r(t)r(t-s)\mathrm{d}t$, $\psi_n = \sum_{\ell\in\mathcal{L}}\mathbb{E}_\tau[I_1^\ell]\sum_{k=1}^{N_p}\mathbb{E}_\tau[I_n^k]$ with $I_n^k = \mathbb{E}_a[(A_n^k)^2]$.

Thanks to Eq. (1), one can see that the MUI can be similarly represented for TH and DS when employing PAM modulation. Consequently the variance given by Eq. (16) remains valid for DS technique.

2) Closed-form expression of $D_M^4 := \mathbb{E}_{a,d,\theta,\tau}[z_M^4]$: the MUI can be decomposed as $z_M = \sum_{n=2}^{N_u} z_{M,n}$ where $z_{M,n} = \sqrt{P_n}\sum_{\ell\in\mathcal{L}} A_1^\ell\sum_{k=1}^{N_p} A_n^k y_{k,\ell,n}(\theta_n)$ is the interference associated with user n. Since the channel amplitude a is zero-mean, the expectation of z_M^4 over a leads to $\mathbb{E}_a[z_M^4] =$

$\sum_{n=2}^{N_u}\mathbb{E}_a[z_{M,n}^4]+6\sum_{\substack{n,m=2\\n\neq m}}^{N_u}\mathbb{E}_a[z_{M,n}^2]\mathbb{E}_a[z_{M,m}^2]$. By using the equality $\sigma_M^2=\sum_{n=2}^{N_u}\mathbb{E}_{a,d,\theta,\tau}[z_{M,n}^2]$, D_M^4 can be expressed as

$$D_M^4=\sum_{n=2}^{N_u}\mathbb{E}_{a,d,\theta,\tau}[z_{M,n}^4]+\frac{3(N_u-2)}{N_u-1}\sigma_M^4,$$

where σ_M^2 is given by Eqs. (16) and (17) for PAM and PPM modulation respectively.
Now, let us focus on the computation of $\mathbb{E}_{a,d,\theta,\tau}[z_{M,n}^4]$ to derive D_M^4. We detail only the computation steps of $\mathbb{E}_{a,d,\theta,\tau}[z_{M,n}^4]$ for PAM modulation. The PPM case can be achieved similarly.

In PAM case, as the time-support of $r(\cdot)$ is much less than T_c, we have $r^p(\epsilon)r^q(\epsilon-T_c)=0$, $\forall p,q$. Consequently, the expectation of $\mathbb{E}_a[z_{M,n}^4]$ over the zero-mean symbol d leads to

$$\begin{aligned}\mathbb{E}_{a,d}[z_{M,n}^4] &= P_n^2\sum_{\substack{k=1\\ell\in\mathcal{L}}}^{N_p}J_1^\ell J_n^k\big[\left(\mathcal{C}_{1,n}^{+4}(q_n^{k,\ell})+\mathcal{C}_{1,n}^{-4}(q_n^{k,\ell})\right)\\ &\times\ r^4(\epsilon_n^{k,\ell})+\left(\mathcal{C}_{1,n}^{+4}(q_n^{k,\ell}+1)+\mathcal{C}_{1,n}^{-4}(q_n^{k,\ell}+1)\right)\\ &\times\ r^4(\epsilon_n^{k,\ell}-T_c)\\ &+\ 6\mathcal{C}_{1,n}^{+2}(q_n^{k,\ell})\mathcal{C}_{1,n}^{-2}(q_n^{k,\ell})r^4(\epsilon_n^{k,\ell})\\ &+\ 6\mathcal{C}_{1,n}^{+2}(q_n^{k,\ell}+1)\mathcal{C}_{1,n}^{-2}(q_n^{k,\ell}+1)r^4(\epsilon_n^{k,\ell}-T_c)\big]\end{aligned}$$

with $J_n^k=\mathbb{E}_a[(A_n^k)^4]$.

The expectation of $\mathbb{E}_{a,d}[z_{M,n}^4]$ over the uniform variable θ_n is obtained by $\mathbb{E}_{a,d,\theta}[z_{M,n}^4]=\frac{1}{T_s}\int_{T_s}\mathbb{E}_{a,d}[z_{M,n}^4]\mathrm{d}\theta$. By writing the integral over $[0,T_s]$ as a sum of integrals over the subinterval $[0,T_c]$, and by taking into account the periodicity of the multiple access codes, we find

$$\begin{aligned}\mathbb{E}_{a,d,\theta}[z_{M,n}^4] &= \frac{\gamma_2}{T_s}P_n^2\sum_{\substack{k=1\\ell\in\mathcal{L}}}^{N_p}J_1^\ell J_n^k\\ &\times\ \sum_{q=0}^{N_c-1}[\mathcal{C}_{1,n}^{+4}(q)+\mathcal{C}_{1,n}^{-4}(q)\\ &+\ 6\mathcal{C}_{1,n}^{+2}(q)\mathcal{C}_{1,n}^{-2}(q)]\end{aligned}$$

with $\gamma_2=\int r^4(t)\mathrm{d}t$. Finally, using previous equalities and averaging $\mathbb{E}_{a,d,\theta}[z_{M,n}^4]$ over the delays $\tau_n^k-\tau_1^\ell$ leads to the following expression for the fourth order moment

$$\begin{aligned}\textbf{PAM format: } D_M^4 &= \frac{\gamma_2}{T_s}\sum_{n=2}^{N_u}P_n^2\phi_n\sum_{q=0}^{N_c-1}\Big[\mathcal{C}_{1,n}^{+4}(q)\\ &+\ \mathcal{C}_{1,n}^{-4}(q)+6\mathcal{C}_{1,n}^{+2}(q)\mathcal{C}_{1,n}^{-2}(q)\Big]\\ &+\ \frac{3(N_u-2)}{N_u-1}\sigma_M^4 \qquad (18)\end{aligned}$$

with $\phi_n=\sum_{\ell\in\mathcal{L}}\mathbb{E}_\tau[J_1^\ell]\sum_{k=1}^{N_p}\mathbb{E}_\tau[J_n^k]$ and σ_M^2 given by Eq. (16).

In PPM modulation case, the expression of the fourth order moment is given by

$$\begin{aligned}\textbf{PPM format: } D_M^4 &= \frac{1}{T_s}\sum_{n=2}^{N_u}P_n^2\Psi_n\sum_{q=0}^{N-1}\Big[(\mathcal{C}_{1,n}^{-4}(q)\\ &+\ \mathcal{C}_{1,n}^{+4}(q))\gamma_3+2(\mathcal{C}_{1,n}^{-3}(q)\mathcal{C}_{1,n}^{+}(q)\\ &+\ \mathcal{C}_{1,n}^{-}(q)\mathcal{C}_{1,n}^{+3}(q))\left(\gamma_3+\gamma_5\right)\\ &+\ 3\mathcal{C}_{1,n}^{-2}(q)\mathcal{C}_{1,n}^{+2}(q)\left(\gamma_3+\gamma_4\right)\Big]\\ &+\ \frac{3(N_u-2)}{N_u-1}\sigma^4 \qquad (19)\end{aligned}$$

with $\gamma_3=\int r_1^2(t)r^2(t)\mathrm{d}t$, $\gamma_4=\int r_1^2(t)r^2(t-\delta)\mathrm{d}t$, $\gamma_5=\int r_1^3(t)r(t-\delta)\mathrm{d}t$, and σ_M^2 given by Eq. (17).

As a conclusion, the AEP for PAM modulation is thus obtained by replacing σ^2 and α in Eq. (12) with Eqs. (13) and (14). Then σ^2 can be expressed via Eq. (16) in terms of multiple access codes, and α is expressed with respect to the multiple access codes through Eqs. (15), (16) and (18). For the PPM modulation, Eq. (16) is replaced with Eq. (17), and Eq. (19) plays the role of Eq. (18).

IV. Multiple access codes minimizing the AEP

Given N_s and the captured powers, the AEP (see Eq. (12)) depends only on α and σ^2. For a given σ^2, one can remark that $\overline{P}_e$ decreases when α increases at high SINR. Therefore, in order to minimize the performance, *i.e.*, the AEP, we have to select the codes that minimize σ^2 and then maximize α. Using Eq. (14) and the monotonic decreasing property of $F^{(-1)}(.)$, maximizing α is equivalent to minimizing D^4 when σ^2 is fixed. Notice that the high SINR assumption is not restrictive since we would like to improve the error floor occuring in the Rake receiver. Due to Eqs. (13)-(19) and the independence of σ_η^2 with respect to the multiple access codes, minimizing σ^2 and D^4 with respect to the multiple access boils down to minimizing σ_M^2 and D_M^4 with respect to the multiple access codes. Unlike the previous sections of this paper where parameters are provided in function of the applied modulation, we need hereafter to distinguish the access techniques for codes selection since the codes belong to $\{0,1\}$ and $\{-1,1\}$ in TH and DS case respectively.

A. Optimal codes in Time Hopping case

Before going further, we introduce the following lemma.

Lemma 1: Let us consider a pair of DTH codes (c_m,c_n) that satisfies $\sum_{q=0}^{N_c-1}(\mathcal{C}_{m,n}^{+}(q)+\mathcal{C}_{m,n}^{-}(q))^2=N_s^2$, then $\sup_q\left(\mathcal{C}_{m,n}^{+}(q)+\mathcal{C}_{m,n}^{-}(q)\right)=1$.
The proof is drawn in Appendix I and uses some results given in [15].

In this subsection, we aim to identify the pair of codes that minimizes both σ_M^2 and D_M^4 given by Eqs. (16) and (18) respectively for PAM modulation, and by Eqs. (17) and (19) respectively for PPM modulation. In [15], it has been proven that a pair of DTH codes minimizes σ_M^2 if and only if $\sum_{q=0}^{N_c-1}\mathcal{C}_{1,n}^{+2}(q)+\mathcal{C}_{1,n}^{-2}(q)=N_s^2$ when PAM modulation is used. Using Lemma 1 and noting that $\mathcal{C}_{1,n}^{-}(q),\ \mathcal{C}_{1,n}^{+}(q)\geq 0$,

we can deduce that

$$\sum_{q=0}^{N_c-1}\left(\mathcal{C}_{1,n}^{+}(q)+\mathcal{C}_{1,n}^{-}(q)\right)^2=N_s^2 \tag{20}$$

is equivalent to $\sum_{q=0}^{N_c-1}\mathcal{C}_{1,n}^{+2}(q)+\mathcal{C}_{1,n}^{-2}(q)=N_s^2$ since $\mathcal{C}_{1,n}^{+p_1}(q)\mathcal{C}_{1,n}^{-p_2}(q)=0,\forall p_1,p_2$. Thus, the codes satisfying Eq. (20) minimize σ_M^2 with PAM modulation. For PPM modulation case, it has been already proven in [15] that a pair of DTH codes minimizes σ_M^2 if and only if $\sum_{q=0}^{N_c-1}\left(\mathcal{C}_{1,n}^{+}(q)+\mathcal{C}_{1,n}^{-}(q)\right)^2=N_s^2$. Now, let us prove that the selected codes (i.e. satisfying Eq. (20)) minimize D_M^4. Inspecting Eqs. (18) and (19) show that D_M^4 is minimum for both PAM and PPM modulations if and only if $\sum_{q=0}^{N_c-1}\mathcal{C}_{1,n}^{+4}(q)+\mathcal{C}_{1,n}^{-4}(q)$ and $\sum_{q=0}^{N_c-1}\mathcal{C}_{1,n}^{+p_1}(q)\mathcal{C}_{1,n}^{-p_2}(q)$ are minimum when $(p_1,p_2)=(2,2)$ with PAM and $(p_1,p_2)=(1,3),(3,1),(2,2)$ with PPM. Reminding that a pair of codes verifying Eq. (20) satisfies $\sum_{q=0}^{N_c-1}\mathcal{C}_{1,n}^{+2}(q)+\mathcal{C}_{1,n}^{-2}(q)=N_s^2$ and $\mathcal{C}_{1,n}^{+p_1}(q)\mathcal{C}_{1,n}^{-p_2}(q)=0,\forall p_1,p_2$. Using Lemma 1, positivity of $\mathcal{C}_{1,n}^{+}(q)$ and $\mathcal{C}_{1,n}^{-}(q)$, we can deduce that $\sum_{q=0}^{N_c-1}\mathcal{C}_{1,n}^{+4}(q)+\mathcal{C}_{1,n}^{-4}(q)$ is minimal as well and is equal to N_s^2. This leads to next Theorem 1 which characterizes the DTH codes minimizing the AEP for PAM and PPM modulations.

Theorem 1: The AEP of user of interest 1 *is minimum for both PAM and PPM modulations, if and only if, the set of pair of DTH codes* $\{(c_1,c_n),\ n=2,\ldots,N_u\}$*, satisfies* $\sum_{q=0}^{N_c-1}\left(\mathcal{C}_{1,n}^{+}(q)+\mathcal{C}_{1,n}^{-}(q)\right)^2=N_s^2$.

Notice that, in [15], the authors suggest to select the DTH codes minimizing the variance. These codes correspond to those that we propose in Theorem 1 when PPM modulation is applied. However, when PAM modulation is used, the codes minimizing the variance only satisfy $\sum_{q=0}^{N_c-1}\mathcal{C}_{1,n}^{+2}(q)+\mathcal{C}_{1,n}^{-2}(q)=N_s^2$ which corresponds to a larger set of codes than the set of codes verifying the condition illustrated in Theorem 1. Consequently in PAM context, the codes minimizing our AEP is only a subset of the codes minimizing the MUI variance.

B. Optimal codes in Direct Sequence case

Before exhibiting the Optimal DS codes, we introduce two preliminary lemmas.

Lemma 2: Let (c_m,c_n) *be two Direct Sequence codes of length* N_c*. We have* $\sum_{q=0}^{N_c-1}\mathcal{C}_{m,n}^{+2}(q)+\mathcal{C}_{m,n}^{-2}(q)\geq N_c$.

Proof of Lemma is given in Appendix II.

Lemma 3: Let (c_1,c_n) *be a pair of DS code satisfying* $\sum_{q=0}^{N_c-1}\mathcal{C}_{1,n}^{+2}(q)+\mathcal{C}_{1,n}^{-2}(q)=N_c$.

- N_c *even case:* $|\mathcal{C}_{1,n}^{+}(q)|=|\mathcal{C}_{1,n}^{-}(q)|=0$ *if* q *is even; and* $|\mathcal{C}_{1,n}^{+}(q)|=|\mathcal{C}_{1,n}^{-}(q)|=1$ *if* q *is odd.*
- N_c *odd case:* $|\mathcal{C}_{1,n}^{+}(q)|=1$, $|\mathcal{C}_{1,n}^{-}(q)|=0$ *if* q *is odd; and* $|\mathcal{C}_{1,n}^{+}(q)|=0$, $|\mathcal{C}_{1,n}^{-}(q)|=1$ *if* q *is even.*

Due to the lack of space, proof of Lemma 3 is omitted. Nevertheless the proof can be done in similar way of those of Lemma 2.

Let $\{(c_1,c_n)\}$ be a set of pair of DS code satisfying Eq. (21). Thanks to Lemma 2, the variance σ_M^2 (given by Eq. (16)) is then minimal. Let us now focus on D_M^4 given by Eq. (18). By means of Lemma 3, one can easily check that $\sum_{q=0}^{N_c-1}\mathcal{C}_{1,n}^{+4}(q)+\mathcal{C}_{1,n}^{-4}(q)$ is minimal and is equal to N_c. The second term of D_M^4, given by $\sum_{q=0}^{N_c-1}\mathcal{C}_{1,n}^{+2}(q)\mathcal{C}_{1,n}^{-2}(q)$, is equal to $N_c/2$ if N_c is even and 0 otherwise, and thus identical for any code minimizing the variance. Therefore, Eq. (21) leads to the joint minimization of σ_M^2 and D_M^4. The proof of the reverse implication can be easily done by using Lemmas 2 and 3. We are now able to state the following Theorem that provides the characterization of optimal pair of DS codes in PAM and PPM modulations context.

Theorem 2: The AEP of user of interest 1 *is minimum, if and only if, the set of pair of DS codes* $\{(c_1,c_n),\ n=2,\ldots,N_u\}$*, satisfies*

$$\sum_{q=0}^{N_c-1}\mathcal{C}_{1,n}^{+2}(q)+\mathcal{C}_{1,n}^{-2}(q)=N_c. \tag{21}$$

Unlike TH scheme with PAM modulation, we see that minimizing jointly the GGD variance and shape parameter is equivalent to minimizing the variance only, in DS scheme context with PAM modulation.

V. Asymptotic distribution of optimal pairs

The optimal codes distribution has been empirically examined in [15] for TH UWB systems. By means of exhaustive search for reasonable values of N_s and N_c, it has been observed in [15] that the percentage of optimal pairs grows with $N_h=N_c/N_s$ for a fixed N_s. It has been thus conjectured in [15] that, the probability that two codes picked at random form an optimal pair goes to 1 when N_h goes to infinity for a fixed N_s. In this section, we aim to prove this conjecture for TH UWB system and we extend the work to DS UWB system case. Let us denote π the probability that a pair of codes (c_1,c_n) is optimal and let us focus on the variation of π in function of the access code parameters, i.e. N_c and N_s for TH technique and $N_c=N_s$ for DS technique.

A. Proportion of optimal pair of codes in Time Hopping case

Reminding that we have proven in section IV-A that an optimal pair (c_1,c_n) satisfies $\sup_q\mathcal{C}_{1,n}(q)=1$, with $\mathcal{C}_{1,n}(q)=\mathcal{C}_{1,n}^{+}(q)+\mathcal{C}_{1,n}^{-}(q)$. Thus, we can define the probability π as follows:

$$\pi:=\Pr\{\forall q\in\{0,\ldots,N_c-1\}\ /\ \mathcal{C}_{1,n}(q)\leq 1\}. \tag{22}$$

Before illustrating the variation of π wrt N_s and N_c, we introduce a new way of interpreting $\mathcal{C}_{1,n}(q)$ that will be useful in the following. Let us start with an example in order to facilitate the understanding where the Time Hopping (TH) codes $\tilde{c}_m$ of length N_s are considered instead of the DTH codes c_m of length N_c. The values of the sequence $\tilde{c}_m$ are drawn in $\{0,\cdots,N_h-1\}$ and the relationship between the two code presentations (TH and DTH codes) is given in [15]. Remind that $\tilde{c}_m(j)$ provides the position of the occupied chip within the j^{th} frame. Let us consider $N_h=5$, $N_s=4$, and the two TH codes $\tilde{c}_m=\{2,4,0,1\}$ and $\tilde{c}_n=\{1,1,4,3\}$. The event $\mathcal{C}_{m,n}(q)=2$ occurs when, for a given delay q, two '1' of the first developed code are aligned with two '1' of the

other developed code. In our example, this occurs for instance for $q = 4$. Notice that the gap of bins between the two '1' is equal to 12. In order to formalize the relationship between the collisions and the positions of the '1' in the DTH code, let us define the *distance*:

$$d_m(p,q) := \tilde{c}_m(q) - \tilde{c}_m(p) + (q-p)N_h \tag{23}$$

which represents the number/gap of bins (or distance) between the '1' of frames p and q for the developed code c_m. According to Eq. (8) and the code periodicity, the set of distances to be considered is given by $\mathcal{D} := \{d_m(p,q), 0 \leq p \leq N_s - 1, p + 1 \leq q \leq p + N_s - 1\}$, where the arguments of the DTH code in (23) have to be taken modulo N_s. In our example, the two equal distances that concur to the collision of weight 2 are $d_m(2,4) = \tilde{c}_m(0) - \tilde{c}_m(2) + (4-2)N_h = 2 - 0 + 2 \times 5 = 12$, and $d_n(1,3) = \tilde{c}_n(3) - \tilde{c}_n(1) + (4-2)N_h = 3 - 1 + 2 \times 5 = 12$ as illustrated in Fig. 3.

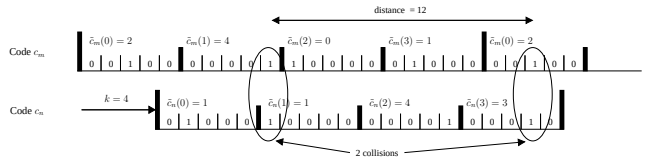

Fig. 3. Example of two pair codes for which two collisions occur ($\mathcal{C}_{m,n} = 2$) for delay $q = 4$

Let us define the event $E_i := \{$it exists at least one value of $q \in \{0, \ldots, N_h - 1\}$ for which $\mathcal{C}_{m,n}(q) = i\}$. Then, we can state that the event E_2 occurs as soon as the two codes have at least one distance in $\mathcal{D}$ equal, and more generally, the event E_i occurs as soon as the two codes have at least $(i-1)i/2$ distances in $\mathcal{D}$ equal. Notice that when the event E_1 occurs, $\mathcal{D}$ may be empty since the notion of *distance* needs at least two collisions. All previous materials will be useful to prove the following Theorem which actually inspects the probability that the event E_1 occurs.

Theorem 3: The probability π, that a pair of DTH code (c_1, c_n) is optimal, is lower bounded by

$$\pi \geq 1 - \frac{N_s(N_s-1)^2}{N_h}\left[N_s - \frac{4}{3} + \frac{1}{3}\left(\frac{1}{N_h}\right)^2\right]. \tag{24}$$

Proof of Theorem 3 is provided in Appendix III. We remark that Theorem 3 confirms the conjecture illustrated in [15]. Indeed, using Eq. (24), it is clear that π converges to 1 when N_h goes to infinity for a given value N_s. Therefore, when TH scheme is used with either PAM or PPM modulation, the probability that two codes picked at random form an optimal pair goes to 1 when N_h is large for a fixed N_s. Moreover, it suggests that for a given N_s, increasing the number of optimal pairs can be done by increasing N_h.

B. Proportion of optimal pair of codes in Direct Sequence case

The distance (23) introduced in the previous case to derive a bound for the probability π is not valid for DS scheme since the code values belong to $\{-1, +1\}$. To find a bound for the probability π, we search to estimate the maximum number of optimal pair of codes. To do this, we examine the optimality conditions for both $\mathcal{C}^+_{1,n}(q)$ and $\mathcal{C}^-_{1,n}(q)$ given in Lemma 3 and we represent them by linear systems of equations with unknown variables $c_n(k)$. The matrix of coefficients is then conditioned by the code c_1. Since the optimality conditions depend on the parity of N_c, we distinguish in the following both cases: N_c is even and N_c is odd.

1) N_c is even: The optimality conditions for $\mathcal{C}^+_{1,n}(q)$ (i.e. $|\mathcal{C}^+_{1,n}(q)| = 0$ if q is even and $|\mathcal{C}^+_{1,n}(q)| = 1$ if q is odd) can be represented by $2^{N_c/2}$ linear systems that differ with the column vector of solutions. These systems are given in Eq. (25).

$$\mathbf{C}_1 \begin{bmatrix} c_n(0) \\ c_n(1) \\ \vdots \\ c_n(N_c-2) \\ c_n(N_c-1) \end{bmatrix} = \underbrace{\begin{bmatrix} \pm 1 \\ 0 \\ \vdots \\ \pm 1 \\ 0 \end{bmatrix}}_{v} \tag{25}$$

with

$$\mathbf{C}_1 = \begin{bmatrix} c_1(N_c-1) & 0 & \cdots & 0 \\ c_1(N_c-2) & c_1(N_c-1) & 0 & 0 \\ \vdots & \vdots & \ddots & \vdots \\ c_1(1) & c_1(2) & \cdots & 0 \\ c_1(0) & c_1(1) & \cdots & c_1(N_c-1) \end{bmatrix}.$$

The $N_c \times 1$ vector of system output v is defined as follows: $v(k) = \pm 1$ if k is even and $v(k) = 0$ otherwise, for $0 \leq k \leq N_c - 1$. The $N_c \times N_c$ matrix of coefficients is the same for all the linear systems with determinant equals to $(c_1(N-1))^{N_c} = 1 \neq 0$. Therefore, each system has at most a unique solution in the N_c variables $c_n(k) \in \{-1, 1\}$, $0 \leq k \leq N_c - 1$, according to the code c_1. Let us denote $S^+(c_1)$ the set of these solutions.

$$\begin{aligned} S^+(c_1) \;=\; & \{c_n \in \{-1,+1\}^{N_c} / \text{ for } 0 \leq q \leq N_c - 1 \\ & |\mathcal{C}^+_{1,n}(q)| = 0 \text{ if } q \text{ is even and} \\ & |\mathcal{C}^+_{1,n}(q)| = 1 \text{ if } q \text{ is odd}\} \end{aligned}$$

Then the cardinality of $S^+(c_1)$ is bounded by $\mathrm{Card}(S^+(c_1)) \leq 2^{N_c/2}$. Now, the representation of the optimality conditions for $\mathcal{C}^-_{1,n}(q)$ (*i.e.* $|\mathcal{C}^-_{1,n}(q)| = 0$ if q is even and $|\mathcal{C}^-_{1,n}(q)| = 1$ if q is odd) with $2^{N_c/2}$ linear systems leads to

$$\mathbf{C}_2 \begin{bmatrix} c_n(1) \\ c_n(2) \\ \vdots \\ c_n(N_c-2) \\ c_n(N_c-1) \end{bmatrix} = \begin{bmatrix} \pm 1 \\ 0 \\ \vdots \\ 0 \\ \pm 1 \end{bmatrix}. \tag{26}$$

where

$$\mathbf{C}_2 = \begin{bmatrix} c_1(0) & c_1(1) & c_1(2) & \cdots & c_1(N_c-2) \\ 0 & c_1(0) & c_1(1) & \cdots & c_1(N_c-3) \\ \vdots & \ddots & \ddots & \ddots & \vdots \\ 0 & \cdots & 0 & c_1(0) & c_1(1) \\ 0 & 0 & \cdots & 0 & c_1(0) \end{bmatrix}$$

and, where the elements of the vector of solutions $\{v(k)\}_{0\leq k\leq N_c-2}$ are equal to $v(k)=\pm 1$ if k is even and $v(k)=0$ otherwise. The matrix of coefficients for each linear system is nonsingular (with non null determinant equals $c_1(0)$), then each system has at most a unique solution in the N_c variables $c_n(k)\in\{-1,1\},\ 1\leq k\leq N_c-1$. Let $S^-(c_1)$ be the set of these solutions:

$$\begin{aligned} S^-(c_1) &= \{c_n\in\{-1,+1\}^{N_c}/ \text{ for } 0\leq q\leq N_c-1 \\ &\quad |\mathcal{C}^-_{1,n}(q)|=0 \text{ if } q \text{ is even and} \\ &\quad |\mathcal{C}^-_{1,n}(q)|=1 \text{ if } q \text{ is odd}\} \end{aligned}$$

The cardinality of $S^-(c_1)$ is then bounded by $\mathrm{Card}(S^+(c_1))\leq 2\times 2^{N_c/2}$. Given a code c_1, a pair of DS code (c_1,c_n) is then optimal if and only if $c_n\in S^+(c_1)\cap S^-(c_1)$. Therefore, the number of optimal pair of codes is at most $2^{N_c/2}$ according to the code c_1. Consequently, as the number of pair of codes is equal to 2^{N_c}, we have $\pi\leq 2^{N_c/2}/2^{N_c}$. Moreover, one can identify a code c_1 that allows to obtain $2^{N_c/2}$ optimal pair of codes. Let c_1 be a DS code whose elements are equal to 1, $c_1(k)=1,\forall k$. By induction, we can easily prove that a code c_n belongs to $S^+(c_1)$, with $c_1(k)=1\ \forall k$, should satisfy $c_n(2k+1)=-c_n(2k),\ \forall k$. Now, let us consider a code c_n belonging to $S^+(c_1)$. Then we can immediately verify that c_n belongs to $S^-(c_1)$ also. Therefore, the number of optimal pair of codes is equal to $\mathrm{Card}(S^+(c_1))=N_c/2$.

2) N_c is odd: By proceeding as for the previous case, we can represent the optimality conditions for $\mathcal{C}^+_{1,n}(q)$ and $\mathcal{C}^-_{1,n}(q)$ with $2^{(N_c+1)/2}$ and $2^{(N_c-1)/2}$ linear systems of equations respectively. The matrices of coefficients are the same as given in Eqs. (25) and (26). The vector of solutions v resembles to that described before where $v(k)=\pm 1$ if k is even and $v(k)=0$ otherwise. However, the vector v that we obtain while considering the optimality conditions for $\mathcal{C}^-_{1,n}(q)$ is different. It satisfies $v(k)=0$ if k is even and $v(k)=\pm 1$ if k is odd. Therefore, the cardinalities of $S^+(c_1)$ and $S^+(c_1)$ satisfy $\mathrm{Card}(S^+(c_1))=\mathrm{Card}(S^-(c_1))\leq 2^{\frac{N_c+1}{2}}$, where $S^+(c_1)$ and $S^-(c_1)$ are the sets of solutions $c_n(k)$ for the linear systems associated with the optimality conditions for $\mathcal{C}^+_{1,n}(q)$ and $\mathcal{C}^-_{1,n}(q)$ respectively. Consequently π is upper-bounded by $2^{(N_c+1)/2}/2^{N_c}$.

Given the comments illustrated in the previous items for the code optimality conditions, we can then state the following Theorem.

Theorem 4: Let us consider a DS UWB system. The probability π to find an optimal pair of codes (c_1,c_n) is bounded by:

$$\pi\leq\begin{cases} 2^{-\frac{N_c}{2}}, & if\ N_c\ is\ even \\ 2^{\frac{1-N_c}{2}}, & if\ N_c\ is\ odd. \end{cases}$$

When N_c is even, it is noticed that it exists at least one code c_1 for which the upper bound for π is achievable.

Unlike TH codes, the proportion of optimal pair of DS codes goes to zero when N_c tends to infinity. Therefore finding optimal codes is often impossible with DS technique whereas it is an easy task with TH technique. This statement is a great advantage for TH technique compared to DS technique.

VI. Numerical results and comparisons

In this section, we compare the empirical Bit Error Rate (BER) and the numerical evaluation of the proposed closed-form expression of the AEP. We also highlight the influence of the codes optimization on the performance (only for PAM in TH context). The analysis concerning the proportion of optimal pair of codes is illustrated as well. Finally we compare TH and DS multiple access techniques and show that the former outperforms the latter.

Let us start by introducing the simulation parameters. We consider a normalized Gaussian impulse

$$w(t)=A_w\sqrt{\frac{2}{\pi}}\frac{\cos(2\pi f_c t)}{\lambda}e^{-\frac{t^2}{2\lambda^2}}$$

with A_w is a normalized factor such that $\int_{-\infty}^{+\infty}w^2(t)\mathrm{d}t=1$, $f_c=6.85$ GHz and $\lambda=9.107\times 10^{-2}$ ns. The captured powers from all the users $\{P_n\}_{n=1,\ldots,N_u}$ are assumed to be equal and they are set to 1. Except otherwise stated, for the sake of simplicity, the considered channel is AWGN. We remind that the generalized Gaussian based modeling holds for multipath channel as shown in Fig 2. For PPM modulation, the delay is set to $\delta=0.0707$ ns.

In Figs. 4 and 5, we compare the theoretical AEP approximation given by Eq. (12) (displayed in solid lines) to the empirical Bit Error Rate (displayed in dotted lines) for different values of N_u in PAM TH, PPM TH systems respectively. The symbol time is equal to $T_s=48$ ns for all systems. The number of chips N_c is equal to 16 and the repetition factor N_s is equal to 4 which means that $N_h=4$.

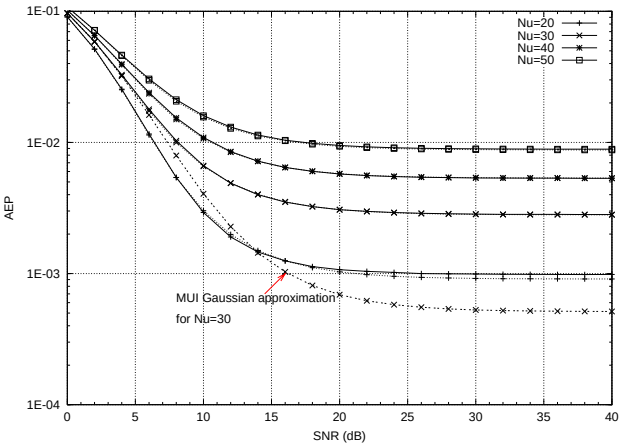

Fig. 4. Theoretical AEP (solid lines) and empirical BER (dotted lines) for PAM TH-UWB system with $N_c=16$, $N_s=4$, $T_c=3$ ns and random codes. AEP with MUI Gaussian approximation for $N_u=30$ (dashed lines).

All figures show the accuracy of our approximation when the codes are chosen at random for the different N_u values, except with PPM modulation where a small gap is noticed with $N_u=20$ and 30. The error probability with the Gaussian approximation ($\alpha=2$ in Eq. (12)) is also plotted in both figures for $N_u=30$. The Gaussian approximation clearly underestimates the error probability for TH UWB and DS UWB systems as already observed in [5].

Let us now examine the impact of the codes optimization on the system performance. We choose a PAM TH-UWB

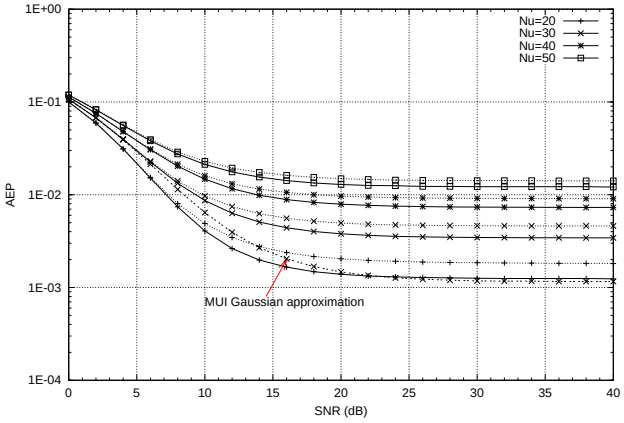

Fig. 5. Theoretical AEP (solid lines) and empirical BER (dotted lines) for PPM TH-UWB system with $N_c = 16$, $N_s = 4$, $T_c = 3$ ns and random codes. AEP with MUI Gaussian approximation for $N_u = 30$ (dashed lines).

system since TH technique guarantees the existence of optimal codes for all the users as proven in Section V and since we will observe difference between codes optimization done with proposed criteria and codes optimization relying on minimization of MUI variance. The number of active users is equal to $N_u = 30$, the symbol time $T_s = 72$ ns, the number of chips is $N_c = 24$ and the repetition factor $N_s = 4$. In Fig. 6, we inspect the impact of the multiple access codes on the performance. For the sake of simplicity, an AWGN channel is considered. We are interesting to three cases: *case 1* corresponds to random codes, *case 2* corresponds to the codes minimizing the MUI variance σ_M^2 as done in [15], and *case 3* corresponds to the codes verifying Eq. (20), *i.e.*, minimizing jointly σ_M^2 and D_M^4.

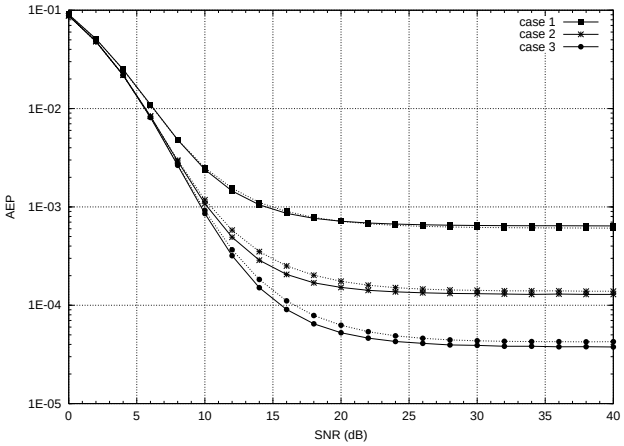

Fig. 6. Theoretical AEP (solid lines) and empirical BER (dotted lines) wrt the codes properties for PAM TH-UWB system with $N_c = 24$, $N_s = 4$, $T_c = 3$ ns and $N_u = 30$.

By comparing these different cases, we notice that the last case leads to the best performance. The selection of the codes that minimize only the variance does not guarantee a minimal error probability. These codes nevertheless improve the performance with respect to the random codes. In Fig. 7, similar curves have been plotted in the following multipath environment: the considered multipath channel is the CM2 model [16] with one cluster. The PRake (Partial Rake) is employed where the receiver uses the first L_r paths among the all N_p received paths. The number of fingers and the paths are fixed to $L_r = 3$ and $N_p = 20$ respectively.

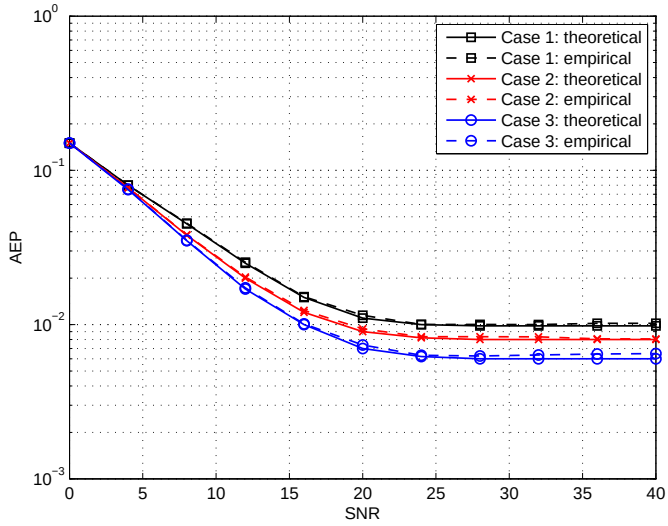

Fig. 7. Performance wrt the codes properties for PAM TH-UWB system in multipath channel with $N_c = 24$, $N_s = 4$, $T_c = 3$ ns and $N_u = 30$.

The improvement achieved thanks to codes optimization is not significant for multipath channel. Indeed, the interference remains important even with the use of optimal codes because of the contribution of each interferer with N_p paths.

In Tab. I.a (resp. Tab. I.b), we estimate π and the number of found optimal pairs N_o for $N_s = 3$ (resp. for $N_s = 6$) using 10^6 random trials (resp. 5×10^6 random trials). We remark that π goes to 1 when N_c increases, but one can also remark that the convergence is slower for $N_s = 6$. This behavior is

TABLE I

ESTIMATED PROBABILITY $\hat{\pi}$ OF π VS N_c FOR $a)$ $N_s = 3$ AND $b)$ $N_s = 6$ IN TH CONTEXT

$a)$ $N_s = 3$ (10^6 trials)

N_c	20	30	40	100	1000
N_o	67579	77329	82311	92802	99256
$\hat{\pi}$	0.67579	0.77329	0.82311	0.92802	0.99256

$b)$ $N_s = 6$ (5×10^6 trials)

N_c	200	600	800	1000	2000
N_o	326417	434097	450140	459936	479223
$\hat{\pi}$	0.652834	0.868194	0.910008	0.919872	0.958446

in accordance with the bound expression (24) which shows that for a given N_c the bound is an increasing function with respect to N_s. Lastly, even when π is far from 1, the number of optimal pair found N_o can be very large and sufficient enough for practical systems with a few tenth of users.

In Fig. 8, we plot both the theoretical upper bound and the empirical percentage of optimal codes in function of

the number of chips per symbol N_c for DS multiple access technique. The figure confirms our theoretical analysis.

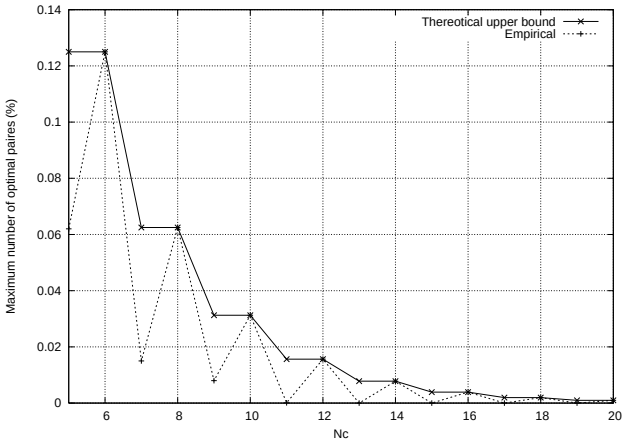

Fig. 8. Estimated probability $\hat{\pi}$ of π vs N_c in DS context

Notice that for N_c even, the bound is reached as mentioned in Theorem 4 whereas for N_c odd, the bound is clearly not achieved. The percentage of optimal codes is rapidly close to zero when N_c is odd ($N_c \geq 13$) while the number of optimal codes approaches zero for $N_c \geq 20$ when N_c is even. Consequently, unlike TH multiple access technique, assigning optimal codes for all active users will be often impossible.

Thanks to numerical results, we have shown that the closed-form expression given by Eq. (12) well approximates the error probability for both TH UWB and DS UWB systems. Therefore, this approximation can be used as a metric to select not only the best codes but also the best access technique which minimizes the error probability. In order to compare both multiple access techniques fairly, we choose the same repetition factor N_s as well as the same symbol time T_s for TH and DS UWB systems. These conditions ensure to obtain the same captured energy as well as the same rate for both systems. Notice that the captured energy is equal to $U = N_s^2 E_w^2 \varphi$ with $E_w = \int w^2(t)\mathrm{d}t = 1$ and φ depends on the channel parameters. For simulations, we take $N_s = 6$, $T_s = 108$ ns and $N_h = 6$ with TH technique. To optimize the performances for both systems, we select the codes in such a way to maximize the number of optimal pair of codes. By simulations, we remarked that we are able to assign optimal codes for all users with TH technique whatever $N_u \leq 64$. However, at most 20% of active users with DS technique use optimal codes. This observation is yet illustrated in Section V where we have proven that the number of optimal DS codes should decrease when increasing N_s. In Fig. 9, we depict the AEP at SNR=30 dB for PAM TH and PAM DS UWB systems in function of the number of users N_u. We add another curve in which we consider that all users with DS technique have optimal codes. This curve can be only obtained using the AEP by forcing the criteria σ_M^2 and D_M^4 to take their minimal values. For the simulated N_u ranges, it is clear that TH scheme gives better performance than DS access technique. Notice that the property on the percentage of optimal pair of codes is crucial to compare properly both multiple access technique. Indeed, if we assume that all users have optimal codes (which is not true for DS technique), then DS technique should be better than TH technique.

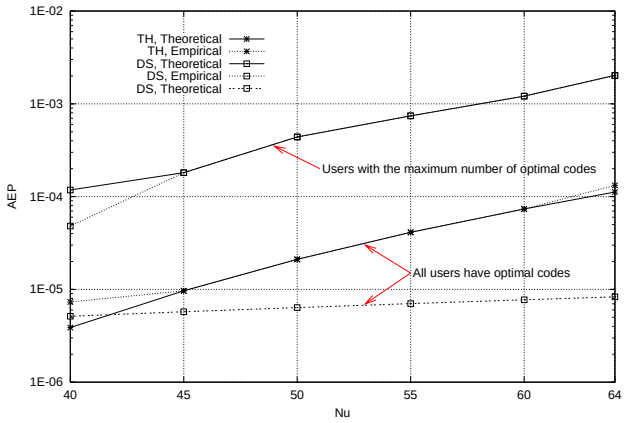

Fig. 9. Comparison of PAM TH-UWB and PAM DS-UWB systems in AWGN channel for $N_s = 6$, $T_s = 108ns$ and $\mathrm{SNR} = 30dB$. Theoretical AEP (solid lines) and empirical BER (dotted lines).

VII. Conclusions

An accurate error probability approximation for PAM TH, PPM TH and PAM DS IR-UWB systems has been derived assuming the MUI distribution is well modeled by GGD for any set of fixed multiple access codes. Based on this approximation, we have deduced the criterion that the multiple access codes have to satisfy in order to minimize the error probability for the three inspected UWB systems. Given this criterion, we have then focused on the percentage of the optimal pair of codes for both TH and DS access technique. Unlike DS scheme, we have proven that TH scheme guarantees to obtaining sufficiently optimal pair of codes when increasing the number of chips per frame N_h for a fixed repetition factor N_s. Numerical results have been depicted to highlight the significant gains while selecting the appropriate codes in TH context. The comparison of TH and DS scheme in AWGN channel using the simulation results shows that the former offers better performance than the latter.

Appendix I
Proof of Lemma 1

Let us denote $\chi_{m,n} = \sum_{j=0}^{N_c-1} \mathcal{C}_{m,n}^2(j)$, where $\mathcal{C}_{m,n}(j) = \mathcal{C}_{m,n}^+(j) + \mathcal{C}_{m,n}^-(j)$. By expressing $\chi_{m,n}$ as in Eq. (27) of [15], $\chi_{m,n} = \sum_{i=1}^{N_s} i^2 \cdot \pi_i$ with $\pi_i \geq 0$ is the number of times that $\mathcal{C}_{m,n}(j) = i$, and by using proposition 3 of [15], we can deduce that $\chi_{m,n} = N_s^2 \Rightarrow \pi_1 \neq 0$ and $\{\pi_i = 0\}_{i=2}^{N_s} \Leftrightarrow \sup_q \mathcal{C}_{m,n}(q) = 1$. For the reverse, we use $\sup_q \mathcal{C}_{m,n}(q) = 1 \Leftrightarrow \pi_1 \neq 0$ and $\{\pi_i = 0\}_{i=2}^{N_s}$, and the proposition 1 of [15], we obtain $\chi_{m,n} = \pi_1 = N_s^2$. ■

Appendix II
Proof of Lemma 2

Given Eq. (8), we show that $\mathcal{C}_{m,n}^-(q)$ and $\mathcal{C}_{m,n}^+(q)$ consist of q and $N_c - q$ terms respectively. Each term belongs to $\{\pm 1\}$.

When N_c is odd, q and $N_c - q$ does not have the same parity. Consequently, when q is even, $\mathcal{C}^-_{m,n}(q)$ is lower-bounded by 0 and $\mathcal{C}^+_{m,n}(q)$ is lower-bounded by 1 which implies that $\mathcal{C}^{+2}_{m,n}(q) + \mathcal{C}^{-2}_{m,n}(q)$ is lower-bounded by 1. When q is odd, we just have to permute the role of $\mathcal{C}^-_{m,n}(q)$ and $\mathcal{C}^+_{m,n}(q)$. Then we deduce immediately that $\sum_{q=0}^{N_c-1} \mathcal{C}^{+2}_{m,n}(q) + \mathcal{C}^{-2}_{m,n}(q)$ is lower bounded by N_c the number of terms in the sum. When N_c is even, similar proof can be done. ■

Appendix III
Proof of Theorem 3

In order to prove Eq. (24), we derive an upper bound for the contrary event $\bar{\pi} := 1 - \pi$.

$$\begin{aligned} \bar{\pi} &= \Pr\{\exists q \in \{0, \dots, N_c - 1\} \ / \ \mathcal{C}_{m,n}(q) \geq 2, \} \\ &= \Pr\{\bigcup_{i=2}^{N_s} \mathcal{C}_{m,n}(q) = i, \forall q\}. \end{aligned} \quad (27)$$

Thanks to the Union Bound (UB), we upper bound (27) as follows:

$$\bar{\pi} \leq \sum_{i=2}^{N_s} \pi_i, \quad (28)$$

where

$$\pi_i := \Pr\{E_i\}. \quad (29)$$

The realization of event E_2 is equivalent to finding two pairs (p_1, q_1) and (p_2, q_2) for which $d_m(p_1, q_1) = d_n(p_2, q_2)$, while the realization of event E_3 is equivalent to the intersection of three sub-events $E_3 = \{E_3^1 \cap E_3^2 \cap E_3^3\}$ with $E_3^1 := \{\exists (p_1, q_1), (p_2, q_2) / \ d_m(p_1, q_1) = d_n(p_2, q_2)\}$, $E_3^2 := \{\exists (p_1, r_1), (p_2, r_2) / \ d_m(p_1, r_1) = d_n(p_2, r_2)\}$, and $E_3^3 := \{\exists (q_1, r_1), (q_2, r_2) / \ d_m(q_1, r_1) = d_n(q_2, r_2)\}$. From basic probability property we have, $\forall i$, $\Pr\{E_3\} \leq \Pr\{E_3^i\}$. Thus, noticing that E_2 and E_3^i are equivalent since they represent the same event, we have proved that $\pi_2 \geq \pi_3$. By recurrence, we can easily extend this results to $\pi_2 \geq \pi_i$, for $i = 3, \dots, N_s$. Consequently, applying those inequalities to Eq. (28) gives:

$$\bar{\pi} \leq (N_s - 1)\pi_2. \quad (30)$$

Using the interpretation of the distance notion introduced in Section V-A, we can re-express π_2 as $\pi_2 = \Pr\{\bigcup_{p_2,q_2}^{p_1,q_1} d_m(p_1, q_1) = d_n(p_2, q_2)\}$. Then, using the UB, π_2 can be upper bounded by S:

$$\pi_2 \leq S := \sum_{\substack{p_1,q_1 \\ p_2,q_2}} \Pr\{d_m(p_1, q_1) = d_n(p_2, q_2)\}. \quad (31)$$

In order to compute S, we consider the codes as random, with values $\tilde{c}_m(q)$ independent and equally distributed in $\{0, \cdots, N_h - 1\}$, and thus $\forall i \in \{0, \cdots, N_h - 1\}$, $\Pr\{\tilde{c}_m(q) = i\} = 1/N_h$. Following those hypothesis and using Eq. (23), we can re-express S as:

$$S = \sum_{\substack{p_1,q_1 \\ p_2,q_2}} \Pr\{\Delta_m - \Delta_n = ((q_2 - p_2) - (q_1 - p_1))N_h\}. \quad (32)$$

with $\Delta_m := \tilde{c}_m(q_1) - \tilde{c}_m(p_1)$. Note that in Δ_m, the dependency to p_1 and q_1 has been removed because of the independence between $\tilde{c}_m(q)$. The same argument applies for Δ_n. Noticing that $(q_2 - p_2) - (q_1 - p_1)$ takes several times the same value over the domain of index variation, we can re-express Eq. (32) as:

$$S = \sum_{\ell=-2N_s+2}^{2N_s-2} \Pr\{\Delta_m - \Delta_n = \ell N_h\} \cdot N_s(N_s - 1)(N_s - |\ell| - 1). \quad (33)$$

Since $\tilde{c}_m(q)$ are drawn in $\{0, \cdots, N_h - 1\}$, $(\Delta_m - \Delta_n)$ varies in $[-2N_h + 2, 2N_h - 2]$. Thus, for $|\ell| \geq 2$, probabilities in the sum (33) are null, and thanks to the symmetrical distribution of $\Delta_m - \Delta_n$, Eq. (33) reduces to:

$$S = N_s(N_s - 1)[\alpha(N_s - 1) + 2\beta(N_s - 2)], \quad (34)$$

with $\alpha := \Pr\{\Delta_m - \Delta_n = 0\}$ and $\beta := \Pr\{\Delta_m - \Delta_n = N_h\}$. Quantity α can be computed as follows:

$$\begin{aligned} \alpha &= \Pr\{\bigcup_{q=-N_h+1}^{N_h-1} (\Delta_m = q) \cap (\Delta_n = q)\} \\ &= \sum_{q=-N_h+1}^{N_h-1} \Pr\{\Delta_m = q\} \Pr\{\Delta_n = q\}. \end{aligned} \quad (35)$$

From $\tilde{c}_m(q)$ probability distribution, straightforward computation gives $\Pr\{\Delta_m = i\} = (N_h - |i|)/(N_h)^2$, which inserted into (35) gives:

$$\alpha = \frac{1}{N_h^2} + 2 \sum_{q=1}^{N_h-1} \frac{(N_h - q)^2}{(N_h)^4} = \frac{2}{3(N_h)} + \frac{1}{3(N_h)^3} \quad (36)$$

Quantity $\beta = \Pr\{\bigcup_{q=1}^{N_h-1} (\Delta_m = q) \cap (\Delta_n = q + N_h)\}$ can be computed as follows:

$$\begin{aligned} \beta &= \sum_{q=1}^{N_h-1} \Pr\{\Delta_m = q\} \Pr\{\Delta_n = q + N_h\} \\ &= \frac{1}{N_h^4} \sum_{q=1}^{N_h-1} (N_h - q)N_h = \frac{1}{6N_h} - \frac{1}{6N_h^3}. \end{aligned} \quad (37)$$

Combining Eqs. (34), (36), and (37) gives:

$$S = N_s(N_s - 1) \left[\frac{N_s}{N_h} - \frac{4}{3N_h} + \frac{1}{3N_h^3} \right]. \quad (38)$$

Thus, we deduce from Eqs. (29), (30), (31), and (38) that $\bar{\pi} \leq \frac{N_s(N_s-1)^2}{N_h} \left[N_s - \frac{4}{3} + \frac{1}{3N_h^2} \right]$, which shows that $\lim_{N_c \to \infty} \bar{\pi} = 0$ and then proves (24). ■

References

[1] M.L. Welborn, "System considerations for ultra-wideband wireless networks," *in Proc. IEEE Radio and Wireless Conf.*, pp. 5-8, Aug. 2001.

[2] M.Z. Win and R.A. Scholtz, "Ultra-wide bandwidth time-hopping spread spectrum impulse radio for wireless multiple-access communications," *IEEE Trans. on Commun.*, vol. 48, no. 4, pp. 679-691, April 2000.

[3] V.S. Somayazulu, "Multiple access performance in UWB systems using time hopping versus direct sequence spreading," *in Proc. Wireless Commun. & Networking Conf.*, pp. 522-525, March 2002.

[4] A.R. Forouzan, M. Nasiri-Kenari, and J.A. Salehi, "Performance analysis of ultrawideband time-hopping code division multiple access systems: uncoded and coded schemes," *in Proc. Int. Conf. on Commun.*, vol. 10, pp. 3017-3021, June 2001.

[5] G. Durisi and G. Romano, “On the validity of Gaussian approximation to characterize the multiuser capacity of UWB TH-PPM,” *in Proc. Conf. on Ultra Wideband Systems and Technologies.*, pp. 157-162, May 2002.
[6] B. Hu and N.C. Beaulieu, “Accurate performance evaluation of time-hopping and direct-sequence UWB systems in multi-user interference,” *IEEE Trans. on Commun.*, vol. 53, no. 6, pp. 1053-1062, June 2005.
[7] J. Fiorina and D. Domenicali, “Revisiting TH-IR-UWB performance limits dependency on essential system parameters using the Generalized Gaussian Approximation,” *in Proc. Int. Conf. on Ultra-Wideband*, pp. 751-754, Sept. 2007.
[8] J. Fiorina, ”A simple IR-UWB receiver adapted to multi-user interferences,” *in Proc. of Globecom*, San Francisco (USA), Dec 2006.
[9] T. Erseghe, V. Cellini, and G. Dona, ”On UWB impulse radio receivers derived by modeling MAI as a Gaussian Mixture,” *IEEE Trans. on Wireless Communications*, vol. 7, no. 6, pp. 2388-2396, June 2008.
[10] H. El Ghannudi, L. Clavier, and P.A. Rolland, ”Modeling Multiple Access Interference in Ad Hoc Networks Based on IR-UWB Signals Up-Converted to 60 GHz”, *in Proc. of European Conference on Wireless Technologies*, Munich (Germany), Oct. 2007.
[11] N. Beaulieu and B. Hu, ”Soft-limiting receiver structures for Time-Hopping UWB in multiple-access interference,” *IEEE Trans. on Vehicular Technology*, vol. 57, no. 2, pp. 810-818, March 2008.
[12] W. Cao, A. Nallanathan and C.C. Chai, ”A Novel High Data Rate Prerake DS UWB Multiple Access System: Interference Modeling and Tradeoff Between Energy Capture and Imperfect Channel Estimation Effect,” *IEEE Trans. on Wireless Commun.*, vol. 7, no. 9, pp. 3558-3567, Sept. 2008.
[13] A.-L. Deleuze, P. Ciblat, and C.J. Le Martret, ”Inter-Symbol/Inter-Frame Interference in Time-Hopping Ultra Wideband Impulse Radio system,” *in Proc. of IEEE International Conference on Ultra-Wideband*, Zürich (Switzerland), Sept. 2005.
[14] C. Nikias, ”Signal processing with alpha-stable distributions and applications,” Wiley Interscience, 1995.
[15] C.J. Le Martret, A.-L. Deleuze, and P. Ciblat, “Optimal time-hopping codes for multi-user interference mitigation in ultra-wide bandwidth impulse radio,” *IEEE Trans. on Wireless Commun.*, vol. 5, no. 6, pp. 1516-1525, June 2006.
[16] A.F. Molish, J.R. Foerster, and M. Pendergrass, “Channel models for ultrawideband personal area networks,” *IEEE Wireless Commun. Mag.*, vol. 10, Dec. 2003.
[17] R.D. Wilson, R.A. Scholtz, “Comparison of CDMA and modulation schemes for UWB radio in a multipath environment,” in *Proc. Global Commun. Conf.*, vol. 2, pp. 754-758, Dec. 2003.
[18] B. Hu and N.C. Beaulieu, “Exact bit error rate analysis of TH-PPM UWB systems in the presence of multiple-access interference,” *IEEE Commun. Letters*, vol. 7, no. 12, pp. 572-574, Dec. 2003.
[19] G. Durisi and S. Benedetto, “Performance evaluation of TH-PPM UWB systems in the presence of multiuser interference,” *IEEE Commun. Letters.*, vol. 7, no. 5, pp. 224-226, May 2003.
[20] J. Fiorina and W. Hachem, “On the asymptotic distribution of the correlation receiver output for time-hopped UWB signals,” *IEEE Trans. on Signal Processing*, vol. 54, no. 7, pp. 2529-2545, July 2006.
[21] W. Niehsen, “Robust Kalman filtering with generalized Gaussian measurement noise,” *IEEE Trans. on Aerospace and Electronic Systems*, vol. 38, no. 4, pp. 1409-1412, Oct. 2002.
[22] S.M. Kay, *Fundamentals of Statistical Signal Processing: Detection Theory*, Englewood Cliffs: Prentice Hall 1998.